2. *DATA REPORT:* HYDROCELL-95 AND -96 SINGLE-CHANNEL SEISMIC DATA ON THE EASTERN JUAN DE FUCA RIDGE FLANK[1]

Andreas Rosenberger,[2] Earl E. Davis,[3] and Heiner Villinger[2]

ABSTRACT

Roughly 900 km of high-quality single-channel seismic reflection profiles were completed on the eastern flank of the northern Juan de Fuca Ridge in 1995 and 1996 to provide structural context for a variety of geophysical and geochemical investigations of hydrothermal circulation and crustal alteration in this young, thickly sedimented environment. Lines are disposed along five primary transects and several local detailed arrays, with most striking normal to local isochrons. The most northerly transect extends from the ridge axis to a point roughly 150 km east over crust 5 Ma in age, and crosses sites drilled during Ocean Drilling Program Leg 168. A brief description of the profiles is provided, although the primary purpose of this report is to provide the reader full access to the data. Towards this end, we provide all profiles in both unmigrated and migrated SEG-Y formats. We also include files of full-resolution differential Global Positioning System navigation and manually picked traveltimes to seafloor and basement reflections.

INTRODUCTION

Through a wide range of studies beginning with the classic *RV Pioneer* magnetics survey (Raff and Mason, 1961), the Juan de Fuca Ridge and flank has become one of the most thoroughly studied areas in the oceans, effectively a type-area for seafloor spreading and related processes. Over the past decade, a great deal of effort has been devoted to the study of ridge-flank hydrothermal circulation on the eastern flank of the ridge, because many simple examples of typical hydrologic regimes as defined by basement structure and sediment cover occur in this relatively small and accessible region. Geophysical and geochemical studies have employed submersibles for fluid sampling from seafloor springs (e.g., Mottl et al., 1998), piston and gravity coring for interstitial fluid sampling (Wheat and Mottl, 1994), heat-flow probes for thermal studies (Davis et al., 1992), multichannel seismic reflection and ocean-bottom seismometer seismic refraction for crustal lithology and physical properties determination (Hasselgren and Clowes, 1995; Rohr, 1994; Rohr et al., 1994), and Ocean Drilling Program (ODP) drilling for deep sediment, rock, and fluid sampling and in situ measurements and monitoring. A brief review of recent work on the eastern flank, including preliminary results of drilling, has been provided by the Shipboard Scientific Party (1997).

Permeability is the primary factor influencing crustal fluid flow, and one of the most fundamental permeability contrasts in the oceanic crust is that between the upper, highly fractured and permeable igneous crust and the hydrologically resistive sediments that bury the igneous rocks progressively with time. Definition of this fundamental hydrologic boundary in oceanic environments relies on high-quality seismic reflection data. Hence, all of the coring, heat-flow, drilling, and numerical modeling studies on the eastern Juan de Fuca Ridge flank have been carried out in the context provided by a number of high-resolution seismic reflection surveys. The importance of this context has been demonstrated clearly in many instances (Davis, Wang, et al., 1997; Fisher and Becker, 1995; Wheat and Mottl, 1994), particularly in the case of studies carried out during and following ODP Leg 168 (Davis and Becker, 1998; Shipboard Scientific Party, 1997).

Although much has been learned in this area, many well-defined problems concerning ridge-flank fluid flow remain to be addressed through additional seafloor and drilling studies. To facilitate planning and provide the structural and hydrologic context for currently ongoing and future studies, we provide in this report single-channel seismic reflection data collected during cruises in 1995 and 1996. These data add considerably to the definition of regional and local sediment thickness and basement depth variations in the region permitted by older single- and multichannel data (e.g., Davis et al., 1992; Rohr et al., 1992; Spence et al., 1990). Complementary heat-flow data collected through 1995 have been published and discussed briefly in Davis, Fisher et al. (1997).

DESCRIPTION OF DATA

Line Locations

Locations of seismic lines are shown in Figures 1 and 2. Five long transects cross the ridge flank out to a distance of roughly 150 km from the ridge axis, where the crustal age is 5 Ma. The direction (typically N 107°E) was chosen to be perpendicular to local magnetically defined isochrons, which in most of the area included by the seismic lines contain no significant offsets associated with fracture zones or propagating rift traces (Currie et al., 1982; Elvers et al., 1972; Wilson 1993; Wilson et al., 1984). The length of the lines was chosen to provide the regional context for detailed heat-flow, coring, and seismic refraction studies in several local areas, and for the Leg 168 drilling transects that extend from roughly 20 to 100 km from the ridge axis. Suites of closely spaced lines and lines parallel to the strike of the ridge axis were collected to provide local structural and hydrologic/lithologic control for the detailed studies.

Seismic Sources

The Hydrocell-95 seismic survey was carried out on board the Canadian *RV John P. Tully* in August 1995. Lines were shot using a single generator-injector (GI) gun, with a reduced volume of 0.74 L (45 in³) for both the generator and the injector chambers. The air compressor sustained 12 MPa (1700 psi) pressure for nominally 10-s shot intervals. The injector firing delay was set to 35 ms throughout the survey.

[1]Fisher, A., Davis, E.E., and Escutia, C. (Eds.), 2000. *Proc. ODP, Sci. Results,* 168: College Station TX (Ocean Drilling Program).

[2]Fachbereich Geowissenschaften, University of Bremen, Postfach 330-440, D-28334 Bremen, Germany. vill@uni-bremen.de

[3]Pacific Geoscience Centre, Geological Survey of Canada, P.O. Box 6000, Sidney, BC V8L 4B2, Canada.

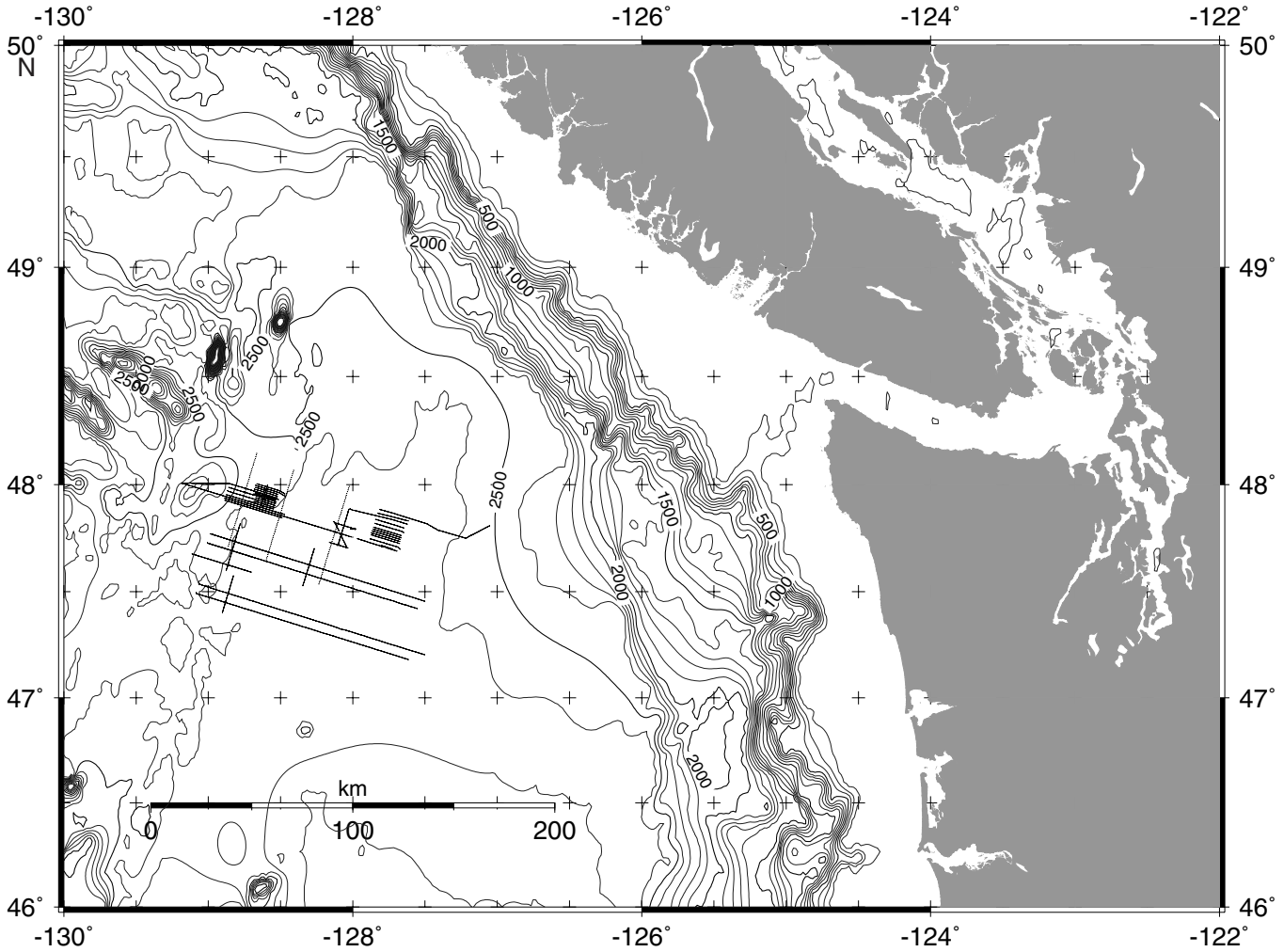

Figure 1. Location map of Hydrocell-95 and -96 seismic lines.

Seismic lines in 1996 were shot from the German research vessel *Sonne* using two GI airguns with a generator chamber volume of 2.9 L (175 in³) and an injector chamber volume of 1.7 L (105 in³). The injector was fired with a delay of 40–48 ms to reduce the bubble oscillations. Operating pressure was 15 MPa (2250 psi), and guns were towed at a depth of 5–6 m.

Hydrophones

A Teledyne array was used in both survey years, with 16 hydrophone groups evenly distributed over 100 m of active length. The tow lead was 120 m long, and the active section was directly coupled with no transformer section. All 16 channels were electrically summed into a single channel.

Acquisition

The custom-built acquisition unit digitized data using two 12-bit analog-to-digital converter channels in combination. One channel was offset in amplification by a factor of 512, then both channels were combined into a single 21-bit data value, yielding a nominal dynamic range of 120 dB (20 bits plus sign). Data were sampled at an initial rate of 2–4 kHz and subsequently decimated. A trigger delay (SEG-Y header-word delrt) was applied according to the two-way traveltime of the seismic signal in the water column.

Navigation

Navigation control was derived from global positioning system data acquired in differential mode (DGPS). In 1996 this was augmented by auxiliary sensors including a Doppler velocity log and gyro compass. Shipboard GPS antenna positions (mounted roughly 15 m forward of the airgun towing point in 1995 and 35 m forward in 1996) were recorded for each shot at the time of the trigger. Trigger signals were derived from the DGPS-determined positions to yield a shot spacing of 25 m along all lines in 1995 and most in 1996. In the instances of Lines 960902a, 05a, and 27a, the airguns were triggered by GPS time once per minute. Ship speed was maintained as steady as possible at about 3 kt to yield a shot spacing of ~100 m along these three lines. Approximate positions for each shot are included in SEG-Y trace headers fields sx, sy, gx, gy, but because SEG-Y navigation keywords do not accommodate the full DGPS precision, separate navigation files are also provided.

Full-precision DGPS navigation data are provided in ASCII files included on CD-ROM Disc 2 in the back pocket of this volume. The DGPS data contains shot times and positions, as well as manually picked two-way traveltimes to the seafloor and to the top of seismic basement. The format for the records of these files (found in the XYZ directory on CD-ROM Disc 2) is shot-#, time-hh, time-mm, time-ss, latitude, longitude, dist-from-ridge, twt-sea-floor, and twt-basement. The day field in the headers of the seismic files is set to the day of the

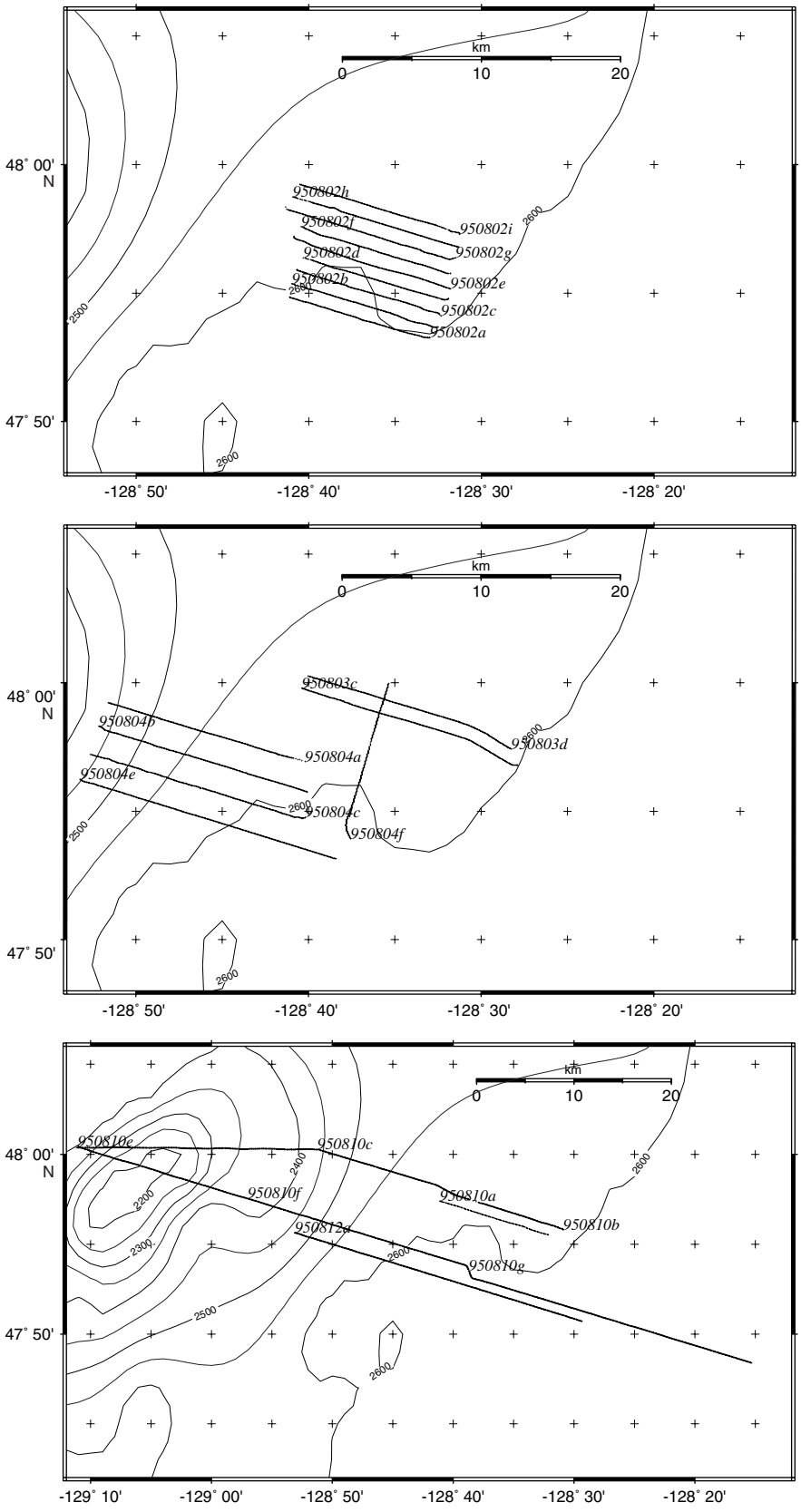

Figure 2. Detailed line locations, with line (and associated file) names given at the beginning of each line.

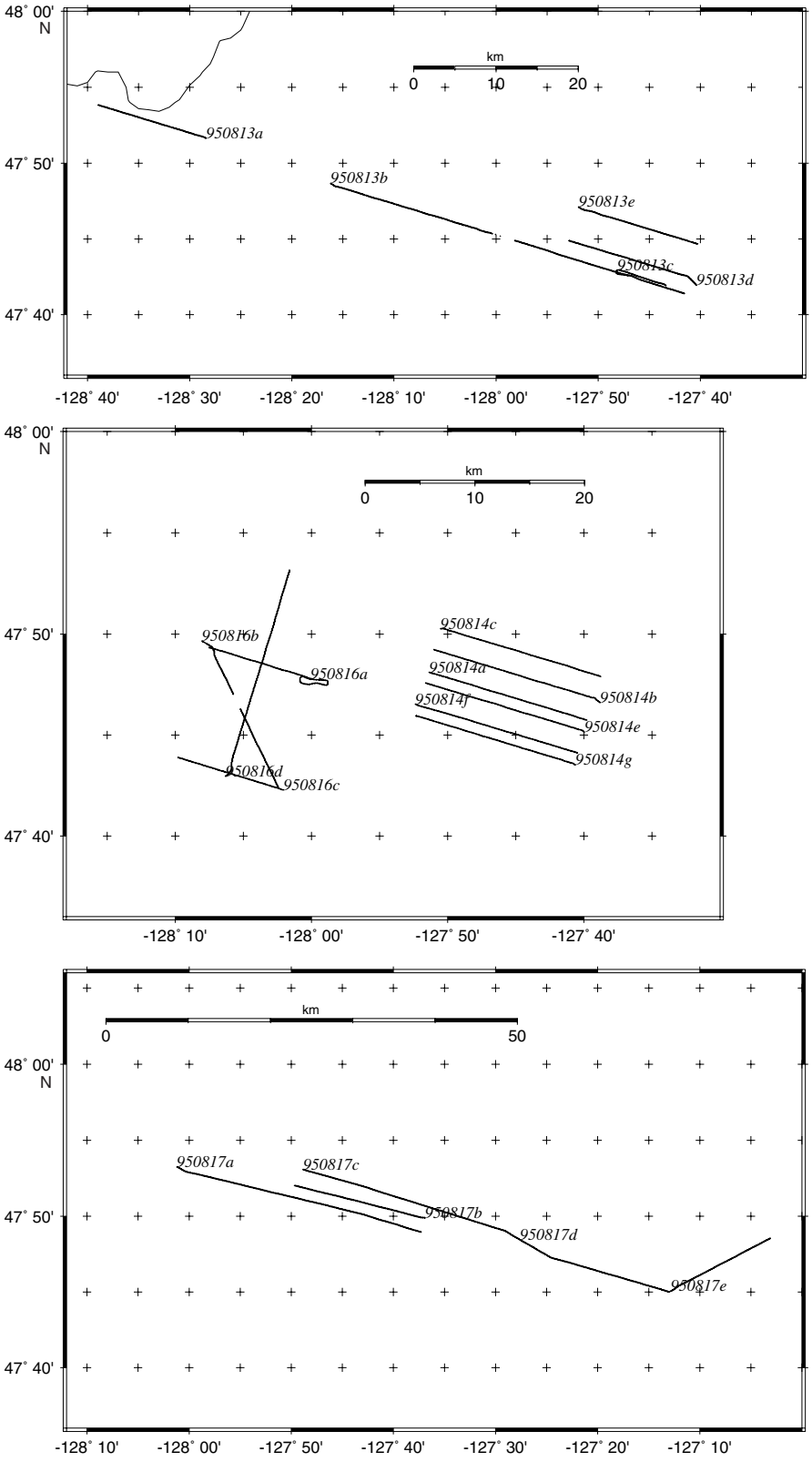

Figure 2 (continued).

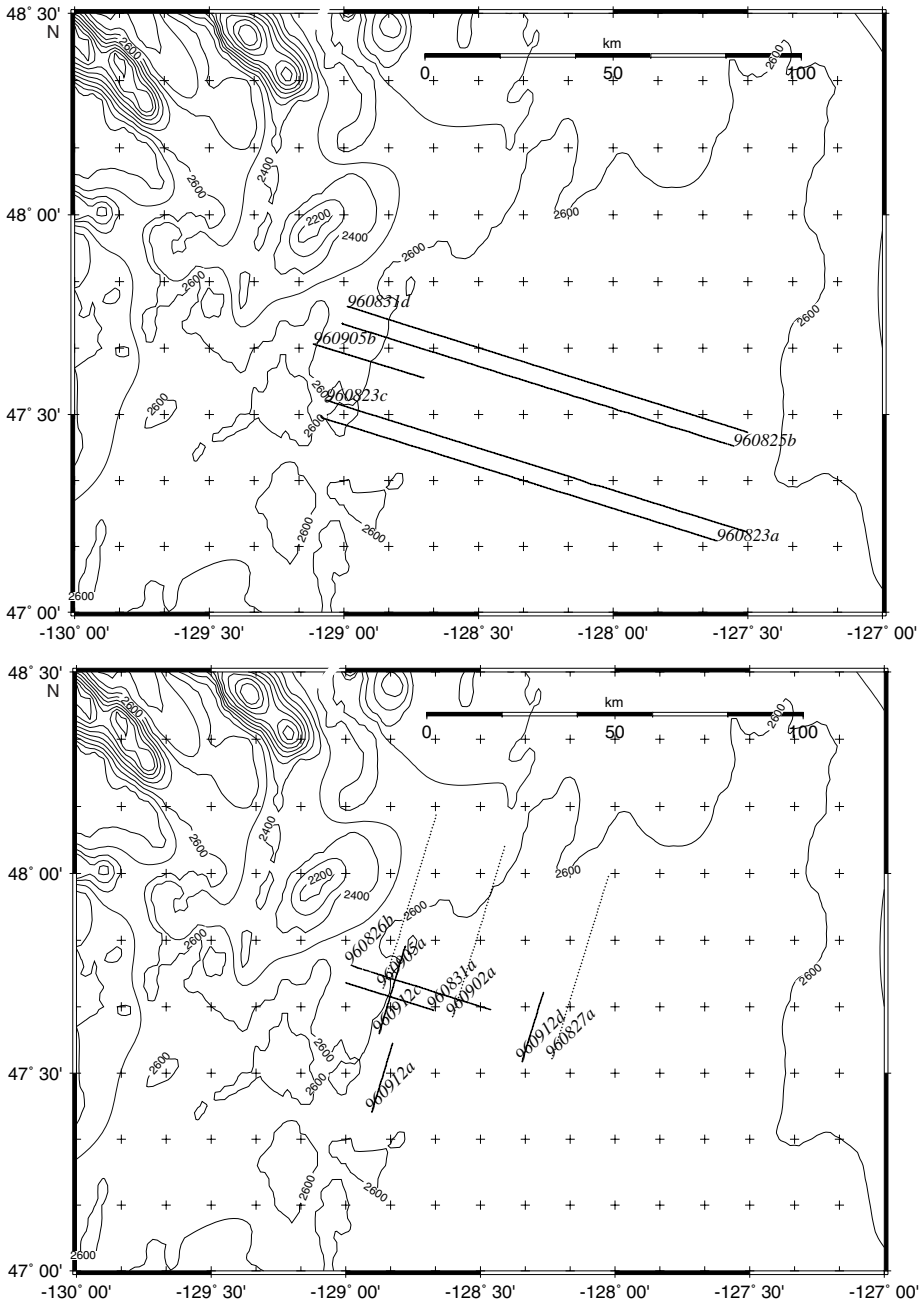

Figure 2 (continued).

month, not to the Julian day as required by SEG-Y. The date on which the profile was started can be read from the filename. For example, file 950804A.XYZ represents data collected from the line initiated on August 4, 1995. Examples showing how reflection times were picked are discussed below. Calculation of distance from ridge is also described below.

Data Processing and Migration

Each line is provided at two different levels of processing. Data in files with name-extension SGY were processed with a bandpass filter and resampled at typically 2-ms sampling intervals. Data in files with name-extension SGM are additionally migrated on a smooth generic velocity-depth function. This velocity-depth function was designed to carry velocities from 1500 m/s at the upper sediments to about 2500–3000 m/s in the basement and is by no means accurate. Because of the great water depth and limited aperture of the seismic system, traveltime migration results are not very sensitive to velocity errors; however, and the quality of the migrated sections is generally very good. Some profiles are additionally dip-filtered after migration to reduce migration noise.

Seismic Data Format

Seismic data are stored in SEG-Y format with an EBCDIC header in individual files with either filename extension sgy (unmigrated data) or sgm (migrated data). These files can be found in the SGY and SGM subdirectories, respectively, on CD-ROM Disc 2 in the back pocket of this volume. File names reflect the date when the line was started. For example, file 950804A.SGM represents data col-

lected from the line initiated on August 4, 1995. Naming convention for the *.SGY, *.SGM, and *.XYZ files has been kept consistent to facilitate matching seismic data and DGPS navigation.

DISCUSSION

Local Structures

Data quality throughout the survey was excellent, and it is anticipated that much can be learned from the profiles directly and through use of the profiles as they provide structural, lithologic, and hydrologic context for other data as discussed above. Two example profiles are provided here that reveal a number of interesting sedimentary lithologic and tectonic features. The profile shown in Figure 3A crosses a broad distributary channel not far from ODP Leg 168 Sites 1026 and 1027. Among the features seen in this profile are (1) locally low-reflection amplitudes in the vicinity of Shot 260 between 3.65 and 3.75 s, equivalent to the interval where unconsolidated massive sands were encountered at Site 1027; (2) the progressive onlap of channel deposits on the levee of the next channel system to the west (between Shots 300 and 400); (3) a normal fault or a differential-compaction growth fault in the lower half of the sedimentary sec-

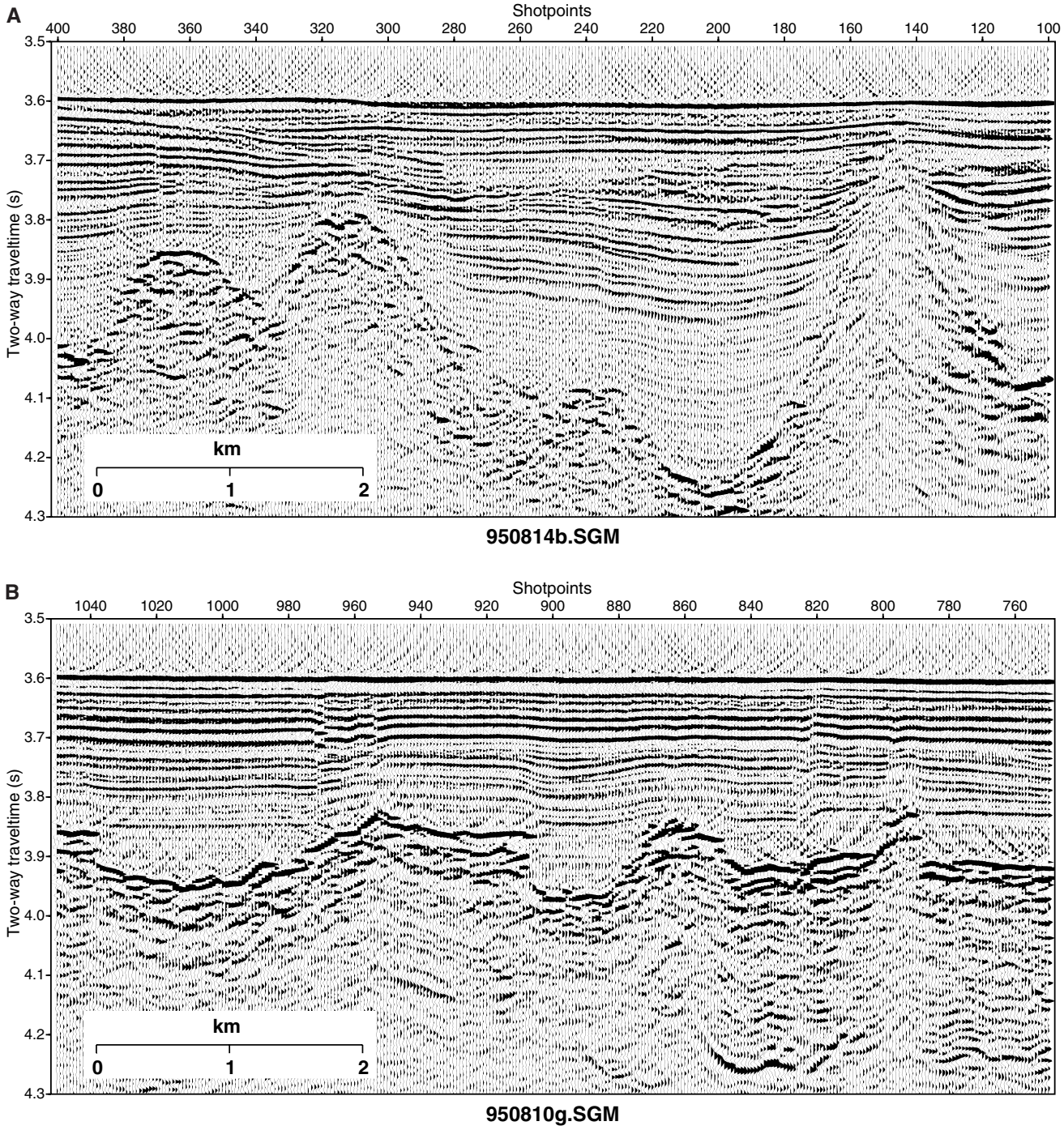

Figure 3. **A–B.** Local examples of relatively common structures that are well resolved by the seismic data.

tion near Shot 240; and (4) a rugged basement surface comprising buried ridges and valleys, with local relief of up to 0.6 s, roughly 600 m. Lower basement relief and a stronger basement reflection amplitude is seen in the profile shown in Figure 3B. Here, some postdepositional deformation of the seismic stratigraphy is clearly related to differential compaction, but several disruptions (e.g., at Shot 820 and near Shot 960) are probably associated with relatively recent off-axis tectonic motion. This section also demonstrates the effectiveness of migration. Sharp offsets in the basement surface produced by normal faulting at the ridge axis or possibly along the edge of intrasedimentary sills or flows erupted off-axis are imaged very well (e.g., near Shots 900 and 1040).

Regional Structure

In addition to local basement and sedimentary structures, the seismic data presented in this report provide constraints on regional basement topography and sediment thickness variations. To facilitate use of the data, we have provided files of manually picked reflection traveltime depths to the seafloor and to the top of seismic basement (format described above). Four "worse-case" examples are provided in Figure 4 to show the nature of potential errors associated with the picks.

Because the seafloor and basement picking were done independently, there are some instances in areas of no sediment cover where depths to the seafloor and to basement differ (Fig. 4A); this can lead to positive and negative small erroneous sediment thicknesses. In areas of rugged basement relief (i.e., where basement is rough, features are small, or the average slope is steep), basement reflections are often weak and difficult to distinguish (Figs. 4B–4D). In many of these instances, the basement surface has been chosen where coherent sedimentary reflectors terminate (Fig. 4B). In the lower parts of thick, older (pre-Pleistocene, nonturbidite) sections, internal reflections are weak, and this method does not work well (Fig. 4C). Where weak basement arrivals approach the seafloor, recognition of basement is made even more difficult by the strong seafloor reflection coda (Fig. 4D). At some locations (e.g., along lines in Figs. 4B and 4D), high-amplitude, reverberant basement reflections may originate from one or more off-axis massive flow units or sills; caution must be used in interpreting these horizons to represent the top of permeable "hydrologic basement" (e.g., Davis and Chapman, 1997).

One of the applications of the data has been to define the regional continuity of the sediment cover on the eastern Juan de Fuca Ridge flank and the local and regional variations in its thickness. Five long transects of seafloor and basement topography derived from the *.XYZ files are shown in Figure 5. The northernmost is a composite (provided for convenience in a single file named LEG_168.XYZ) that crosses the ODP Leg 168 drilling sites (Fig. 5A). Distances shown in the profiles and provided in the *.XYZ files have been determined by projection onto a line striking at N 107°E (perpendicular to the strike of local isochrons) and beginning at the Endeavour ridge axis at 47°58.46´N, 129°4.8´W. Whereas most of the crust along the profiles was created by Endeavour segment spreading, recent northward propagation of the Cobb offset (Johnson et al., 1983) causes complications to the simple age structure in the youngest parts of the southerly profiles (Fig. 5B). Approximate ages along the lines are shown for those portions having a simple spreading history.

Several things contribute to the observed basement topography and sediment distribution. On a large scale, thermal aging and subsidence of the Juan de Fuca Plate along with the effects of sediment loading cause the basement surface to deepen with age. Departures from a simple monotonic and consistent rate of subsidence are evident, both in the way of departures from a smooth basement depth vs. age increase and in a general trend of increasing basement depths to the south over the latitudinal range covered by the profiles. The cross-strike variations may be associated with long-term variations in effective axial lithospheric temperatures and crustal volcanic supply. The along-strike variations may be related to original variations in depth associated with ridge segmentation. On a small scale, topographic relief created by normal faulting and variations in volcanic supply at the rift axis is present (e.g., Kappel and Ryan, 1986). The amplitude of this relief is typically about 100 m, although relief of over 600 m is present in the eastern portion of the northern line. Small seamounts also create local relief, and at five locations, edifices rise above the sediment surface. With the exception of these seamounts and the elevated region lying within about 20 km of the ridge axis, the basement relief is fully buried by flat-lying turbidite sedimentary deposits derived from the nearby continental margin during the Pleistocene.

ACKNOWLEDGMENTS

Many people assisted with the collection and processing of the data presented in this report. We would especially like to thank the captain and crews of the research vessels *Tully* and *Sonne.* The careful review by Suzanne Carbotte is kindly acknowledged. Support for the field programs was provided by the German Ministry for Education and Research (BMBF), Projects 03G0520 and 03G0111A and the Geological Survey of Canada.

REFERENCES

Currie, R.G., Seemann, D.S., and Riddihough, R.P., 1982. Total magnetic field anomaly, offshore British Columbia. *Open File Rep.—Geol. Surv. Can.,* 828.

Davis, E.E., and Becker, K., 1998. Borehole observatories record driving forces for hydrothermal circulation in young oceanic crust. *Eos,* 79:369.

Davis, E.E., and Chapman, D.S., 1997. Problems with imaging cellular hydrothermal convection in oceanic crust. *Geophys. Res. Lett.,* 23:3551–3554.

Davis, E.E., Chapman, D.S., Mottl, M.J., Bentkowski, W.J., Dadey, K., Forster, C., Harris, R., Nagihara, S., Rohr, K., Wheat, G., and Whiticar, M., 1992. FlankFlux: an experiment to study the nature of hydrothermal circulation in young oceanic crust. *Can. J. Earth Sci.,* 29:925–952.

Davis, E.E., Chapman, D.S., Wang, K., Villinger, H., Fisher, A.T., Robinson, S.W., Grigel, J., Pribnow, D., Stein, J., and Becker, K., 1999. Regional heat-flow variations across the sedimented Juan de Fuca Ridge eastern flank: constraints on lithospheric cooling and lateral hydrothermal heat transport. *J. Geophys. Res.*, 104:17675–17688.

Davis, E.E., Fisher, A.T, Firth, J.V., and Shipboard Scientific Party, 1997. Drilling program traces fluid circulation through Juan de Fuca Ridge crust. *Eos,* 19:187.

Davis, E.E., Wang, K., He, J., Chapman, D.S., Villinger, H., and Rosenberger, A., 1997. An unequivocal case for high Nusselt-number hydrothermal convection in sediment-buried igneous oceanic crust. *Earth Planet. Sci. Lett.,* 146:137–150.

Elvers, D., Potter, K., Seidel, D., and Morley, J., 1972. IODE 1971 survey. *Nat. Ocean. Atmosph. Admin., Nat. Ocean Surv. Seamap Profiles,* Plate BGM-1-171.

Fisher, A.T., and Becker, K., 1995. Correlation between seafloor heat flow and basement relief: observational and numerical examples and implications for upper crustal permeability. *J. Geophys. Res.,* 100:12641–12657.

Hasselgren, E.O., and Clowes, R.M., 1995. Crustal structure of northern Juan de Fuca plate from multichannel reflection data. *J. Geophys. Res.,* 100:6469–6486.

Johnson, H.P., Karsten, J.L., Delaney, J.R., et al., 1983. A detailed study of the Cobb offset of the Juan de Fuca Ridge: Evolution of a propagating rift. *J. Geophys. Res.,* 88:2297–2315.

Kappel, E.S., and Ryan, W.B.F., 1986. Volcanic episodicity and a non-steady state rift valley along Northeast Pacific spreading centers: evidence from Sea MARC I. *J. Geophys. Res.,* 91:13925–13940.

Mottl, M.J., Wheat, C.G., Baker, E., Becker, N., Davis, E., Feely, R., Grehan, A., Kadko, D., Lilley, M., Massoth, G., Moyer, C., and Sansone, F., 1998. Warm springs discovered on 3.5 Ma oceanic crust, eastern flank of the Juan de Fuca Ridge. *Geology,* 26:51–54.

Raff, A.D., and Mason, R.G., 1961. Magnetic survey off the west coast of North America 40°N latitude to 50°N latitude. *Geol. Soc. Am. Bull.,* 72:1267–1270.

Rohr, K.M., 1994. Increase of seismic velocities in upper oceanic crust and hydrothermal circulation in the Juan de Fuca plate. *Geophys. Res. Lett.,* 21:2163–2166.

Rohr, K.M.M., Davis, E.E., and Hyndman, R.D., 1992. Multi-channel seismic reflection profiles across Middle Valley, northern Juan de Fuca Ridge. *Open-File Rep.—Geol. Surv. Can.,* 2476.

Rohr, K.M., Schmidt, U., Lowe, C. and Milkereit, B., 1994. Multi-channel seismic reflection profile across Endeavour segment, Juan de Fuca Ridge. *Open-File Rep.—Geol. Surv. Can.,* 2847.

Shipboard Scientific Party, 1997. Introduction and summary: hydrothermal circulation in the oceanic crust and its consequences on the eastern flank of the Juan de Fuca Ridge. *In* Davis, E.E., Fisher, A.T., Firth, J.V., et al., *Proc. ODP, Init. Repts.,* 168: College Station, TX (Ocean Drilling Program), 7–21.

Spence, G.D., Hyndman, R.D., Langton, S.G., Davis, E.E., and Yorath, C.J., 1990. Multichannel seismic reflection profiles across the Vancouver Island continental shelf and slope. *Open-File Rep., Geol. Surv. Can., 2391.*

Wheat, C.G., and Mottl, M.G., 1994. Hydrothermal circulation, Juan de Fuca Ridge eastern flank: factors controlling basement water composition. *J. Geophys. Res.,* 99:3067–3080.

Wilson, D.S., 1993. Confidence intervals for motion and deformation of the Juan de Fuca plate. *J. Geophys. Res.,* 98:16053–16071.

Wilson, D.S., Hey, R.N., and Nishimura, H., 1984. Propagation as a mechanism of reorientation of the Juan de Fuca Ridge. *J. Geophys. Res.,* 90:9215–9225.

Date of initial receipt: 30 November 1998
Date of acceptance: 27 June 1999
Ms 168SR-021

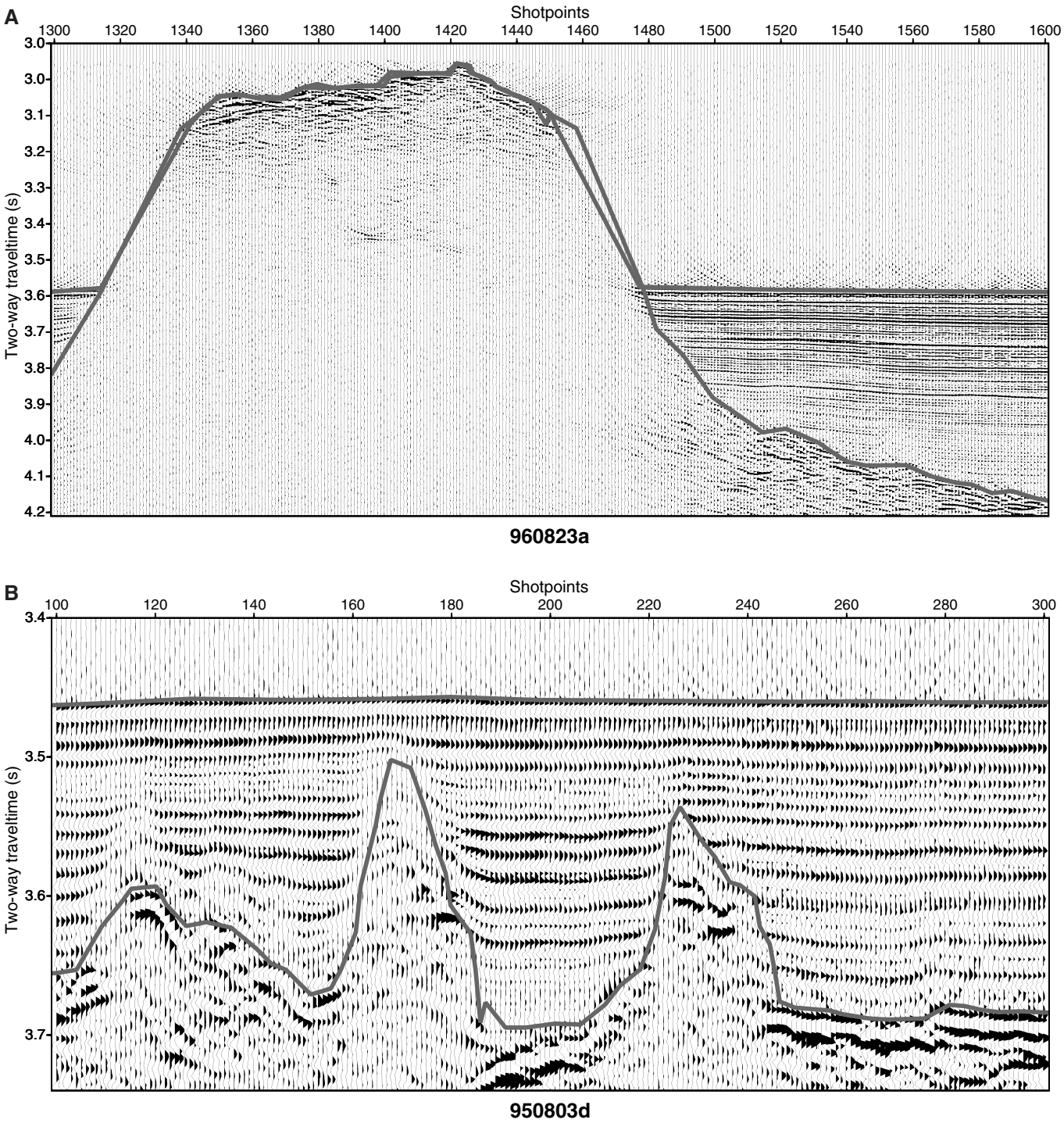

Figure 4. Examples of seafloor and basement picks along four seismic profiles **(A-D)** showing the potential inaccuracies in the *.XYZ files.

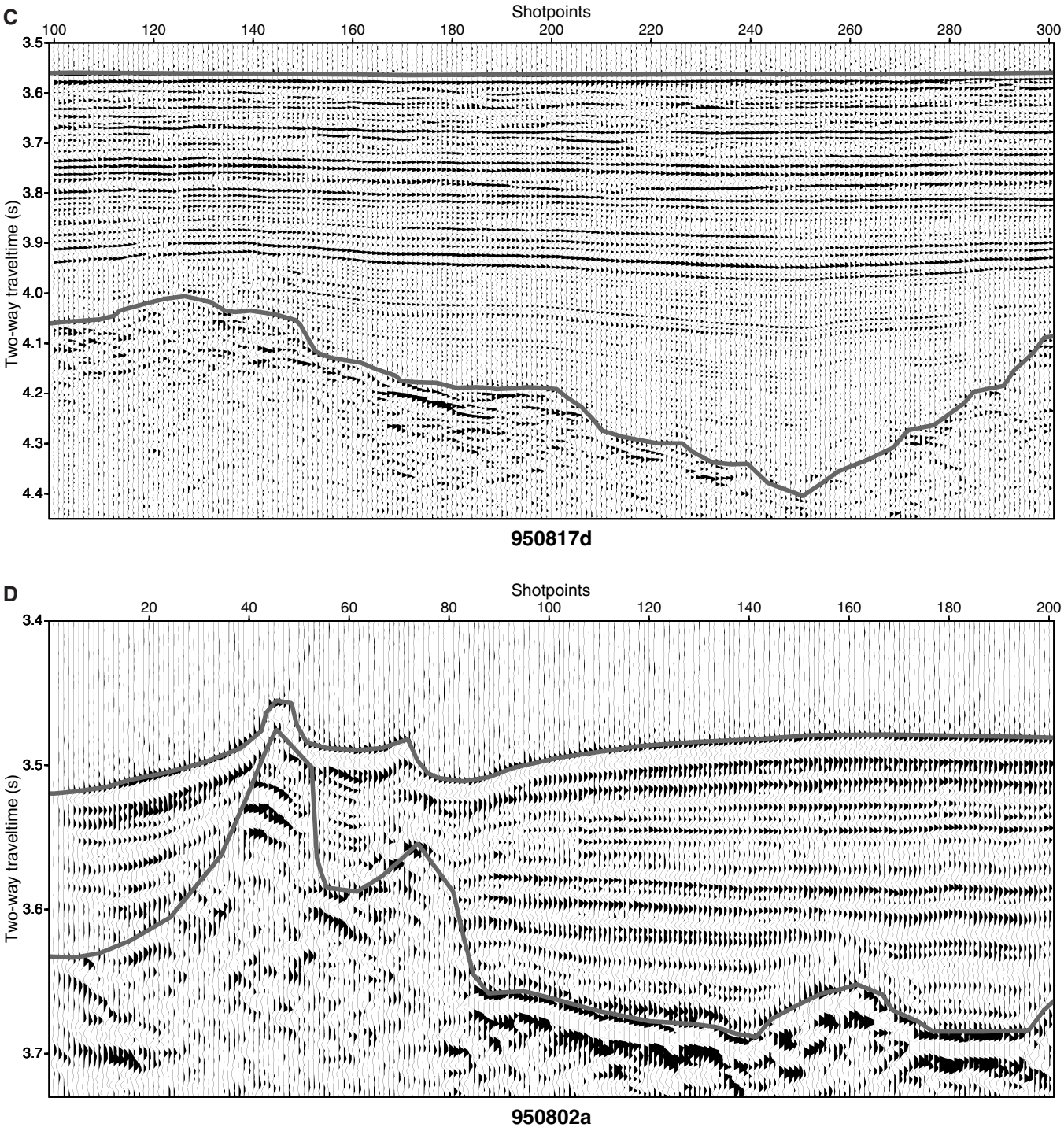

Figure 4 (continued).

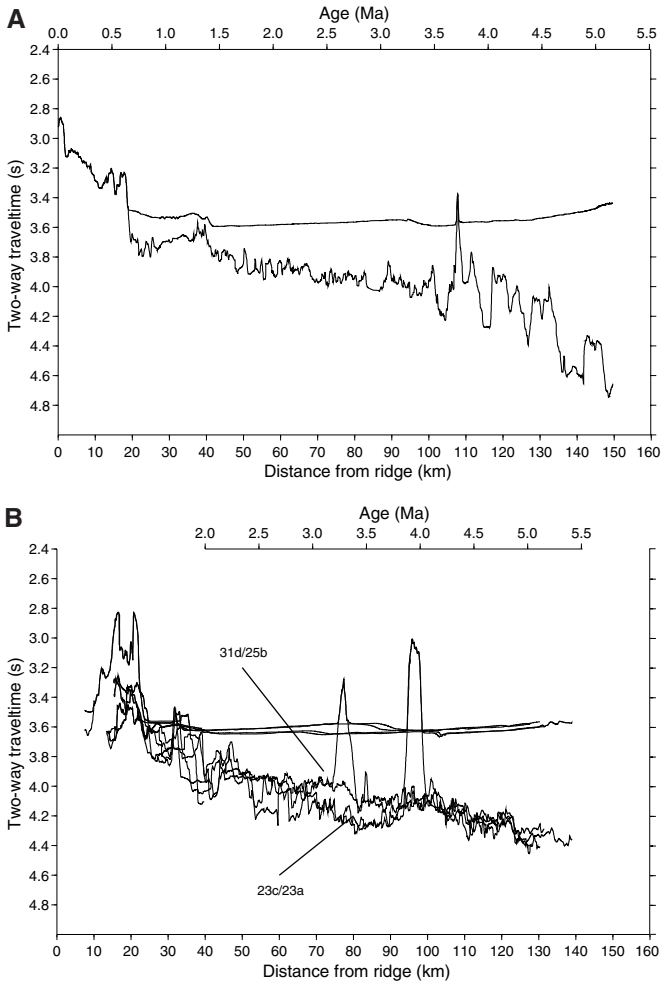

Figure 5. **A–B.** Regional structure as defined by the seafloor and basement data provided in the *.XYZ files. Depths to the seafloor can be estimated from the two-way traveltimes using an average velocity for the water column of 1480 m/s. Subseafloor depths can be estimated using the velocity functions presented in Davis et al. (1999) derived from drill-core velocity measurements and traveltimes and drilled depths to basement.